ORIGINAL RESEARCH PAPER

Fuel Cells DOI: 10.1002/fuce.201400129

High Polymer Content 2,5-Pyridine-Polybenzimidazole Copolymer Membranes with Improved Compressive Properties

M. A. Molleo[1], X. Chen[2], H. J. Ploehn[2], B. C. Benicewicz[1]*

[1] Department of Chemistry and Biochemistry, University of South Carolina, Columbia, SC 29208
[2] Department of Chemical Engineering, University of South Carolina, Columbia, SC 29208

Received August 06, 2014; accepted October 28, 2014; published online November 28, 2014

Abstract

Three series of polybenzimidazole (PBI) random copolymers (2,5-pyridine-r-meta-PBI, 2,5-pyridine-r-para-PBI, and 2,5-pyridine-r-2OH-PBI) were synthesized and cast into phosphoric acid (PA) doped membranes using the PolyPhosphoric Acid (PPA) Process. Copolymer composition was adjusted using co-monomers that impart high and low solubility characteristics to simultaneously control overall copolymer solubility and gel membrane stability. Measured under a static compressive force at 180 °C, copolymer membranes generally exhibited decreased creep compliance with increasing polymer content. Within each series of copolymer membranes, increasing polymer contents proportionally reduced the phosphoric acid/polymer repeat unit (PA/PRU) ratios and their respective proton conductivities. Some copolymer membranes exhibited comparable fuel cell performances (up to 0.66 V at 0.2 A cm^{-2} following break-in) to para-PBI (0.68 V at 0.2 A cm^{-2}) and equal to 3,5-pyridine-based high solids membranes. Furthermore, 2,5-pyridine copolymer membranes maintained a consistent fuel cell voltage of >0.6 V at 0.2 A cm^{-2} for over 8600 h under steady-state operation conditions. Phosphoric acid loss was monitored during long-term studies and demonstrated acid losses as low as 5.55 ng cm^{-2} h^{-1}. The high-temperature creep resistance and long-term operational stabilities of the 2,5-pyridine copolymer membranes suggest that they are excellent candidates for use in extended lifetime electrochemical applications.

Keywords: Creep Compliance, Fuel Cell, Membrane Creep, Meta-PBI, 2OH-PBI, Para-PBI, PBI, PBI Copolymers, PEM, Phosphoric Acid, Polybenzimidazole, Polymer Electrolyte Membrane, PPA Process, Pyridine PBI

1 Introduction

Polymer electrolyte membrane / proton exchange membrane (PEM) fuel cells have been recognized for several decades as efficient energy conversion devices for mobile and stationary applications [1, 2]. Throughout these years, a variety of materials have been responsible for the conversion of chemical energy to electrical energy as polymer electrolytes. Perfluorosulfonic acid (PFSA) PEMs, such as DuPont's Nafion, depend on water clusters to transport protons from anode to cathode; thus, intricate water-management systems and low operational temperatures (<100 °C) are required to keep the membrane properly hydrated. As a result of low operational temperatures, these fuel cells have a low tolerance to fuel impurities.

Polybenzimidazoles (PBIs) have been recognized since the early 1960's as physically, thermally, and chemically robust materials [3, 4]. These polymers were commercialized by Celanese (now PBI Performance Products) for high temperature protective clothing including firefighter turnout coats and astronaut space suits. Additionally, PBIs are processed as high-performance engineering thermoplastics under the trade name Celazole for semiconductor and thermal insulation applications. Over the past twenty years, PBIs have been cast into membranes and doped with PA for electrochemical applications [5–7]. PBIs were first used as PEMs for fuel cells by researchers at Case Western Reserve University in the mid-1990's [5]. A series of separate operations was used to prepare membranes, including polymerization, polymer isolation and dissolution, membrane casting, solvent removal, film washing and drying, and PA doping. This method of membrane fabri-

[*] *Corresponding author, benice@sc.edu*

cation was a time-consuming multistep procedure [5–7]. In addition, the conventional casting technique produced films with relatively low anhydrous proton conductivities (0.048 S cm^{-1} at 180 °C) [6].

The PPA Process provides a simplified pathway to obtain high molecular weight PBI membranes that are fully doped with phosphoric acid and has been optimized and commercialized over the past decade [7–14]. Using a standard reaction vessel equipped with a mechanical stirrer and an inert atmosphere, diacid and tetraamine monomers are reacted using PPA as a solvent. Because PPA is a good solvent for many PBIs, higher molecular weight polymers can be achieved. The rate of the polymerization can be easily controlled by adjusting the stir-rate and the time-temperature profile of the reaction. Upon reaching high molecular weights, the polymerization solution is cast directly into films of uniform thickness. Hydrolysis of the PPA to PA (a poor solvent for many PBIs) causes the film to undergo a sol-to-gel transition, thereby producing a gel membrane fully imbibed with PA. Membranes produced using this method are able to hold higher amounts of phosphoric acid and generate much higher anhydrous proton conductivities (0.10-0.48 S cm^{-1}at 180 °C) than membranes produced by conventional imbibing processes [14]. PA-doped PBI PEMs have been shown to operate at temperatures up to 200 °C with higher tolerances to fuel impurities, and without the need for humidification control [7, 8, 15–17].

Polybenzimidazole (PBI) membranes have garnered much attention over the past decade as viable materials for PEM fuel cells [7, 9, 14, 18]. At high temperatures, PBI-based MEAs display a high resistance to fuel gas impurities such as carbon monoxide and hydrogen sulfide [11, 19, 20]. Their electrochemical durability has been established via shut-down/start-up cycling, phosphoric acid (PA) loss measurements, and long-term steady state operation (>18,000h) [11]. Applications of PBI MEA's in fuel cells include stationary combined heat and power units, mobile power, and range extenders for electric powered vehicles [15].

Little is known about the membrane's resistance to long-term degradation modes including polymer creep and membrane thinning, which can result in gas crossover, voltage degradation, and the eventual quenching of the fuel cell. For stationary fuel cell applications, the Department of Energy has set an operational target of 40,000h for 2015 [21]. A thorough understanding of the long-term degradation modes of PBI MEAs is crucial to design membranes that are resistant to creep and membrane thinning, and meet lifetime requirements. One study concluded that the contact stress in a PBI MEA decreased with time at 180 °C [22]. Investigations of the creep and compression properties of commercially available Nafion membranes at operational temperatures (70–90 °C) have been performed, although these water-based membranes have fundamentally different mechanical issues due to dehydration of the polymer matrix at elevated temperatures [23–25]. Recently, we have initiated studies to investigate the high temperature creep properties in compression since these properties are critical for long-term fuel cell operation [26]. New approaches for improving the long-term mechanical properties of PBI membranes are needed which are cost effective and compatible with the manufacturing processes that have been developed for these unique membrane materials.

It is well known that the PBI chemistry fundamentally affects the processability of the polymer and the properties of the resulting membrane [9, 18]. As described recently, the mechanical properties of PBI membranes can be improved by increasing the polymer content in the gel membrane [26]. However, the solubilities of the copolymers in PPA and viscosities of the resulting PBI/PPA solutions limited the processability of the solutions into films. If the polymer content was too high, the solution became unprocessable either because the polymer could not completely dissolve into the PPA solution, or because the solution became too viscous to cast into a membrane. This limitation was circumvented by synthesizing functionalized PBI copolymers made from a 3,5-pyridinedicarboxylic acid monomer, which imparts higher solubility in the copolymers. Additionally, the effects of chemical structure on both gel thermal stability and electrochemical properties were reported. Figure 1 outlines the relationship between the solubility of some common PBIs in polyphosphoric acid (PPA) and PA and the thermal stabilities of the resulting gel membranes. It was observed that a high ratio of the 3,5-pyridine-PBI moiety in the copolymer correlated with a decrease in thermal stability for the resulting gel membrane. Prior work also showed that 2,5-pyridine-PBI membranes were much more thermally stable than their 3,5-pyridine-PBI membrane counterpart [10]. From these reports, it was hypothesized that a monomer such as 2,5-pyridinedicarboxylic acid (used in place of 3,5-pyridinedicarboxylic acid) could result in copolymer membranes with high polymer content and higher gel thermal stabilities and proton conductivities.

In this work, we report our results on the preparation of novel PPA-processed 2,5-pyridine-r-para-PBI, 2,5-pyridine-r-meta-PBI, and 2,5-pyridine-r-2OH-PBI membranes. The highly

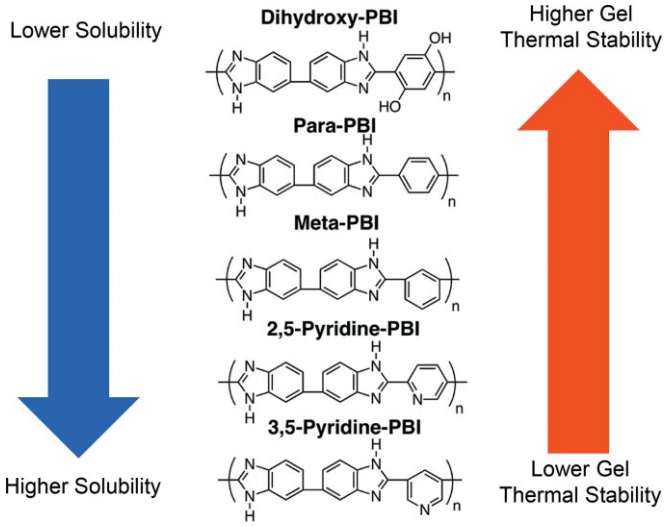

Fig. 1 Relative comparison of PBI chemistries, gel thermal stabilities, and solubilities in PPA and PA.

soluble 2,5-pyridine moiety was used to impart higher polymer solubility in PPA, and therefore, higher polymer content in the membranes. Copolymers of 2,5-pyridine-PBI with either para-, meta-, or 2OH-PBI were prepared and investigated for their relative solubilities and gel membrane stabilities. The high-temperature compressive properties and electrochemical properties of these higher polymer content membranes were measured, which expanded our understanding of the relationships between PBI membrane composition and chemical structures with the fundamental properties of gel stability, membrane conductivity, mechanical properties and fuel cell performance.

2 Experimental

2.1 Chemicals

2,5-Pyridinedicarboxylic acid (2,5-py-2COOH) was purchased from Acros Chemical and TCI America (~98% purity) and purified by recrystallization from a 1:1 dilution of concentrated hydrochloric acid. 2,5-Dihydroxyterephthalic acid (2OH-TPA) was purchased from TCI America and Sigma Aldrich (~98% purity) and purified by recrystallization from a 3:2 dilution of absolute ethanol:water. Terephthalic acid (TPA, purified) and isophthalic acid (IPA, purified) were purchased from Amoco Chemicals. 3,3′,4,4′-Tetraaminobiphenyl (TAB, purified) was donated by BASF Fuel Cell, Inc. Polyphosphoric acid (PPA, 115%) was obtained from InnoPhos, Inc. and stored under nitrogen.

2.2 Polybenzimidazole Synthesis and Membrane Preparation

To synthesize the 2,5-pyridine-based random copolymers, 2,5-py-2COOH and either IPA, TPA, or 2OH-TPA were combined with TBA and PPA in a three-necked flask equipped with nitrogen flow and overhead stirrer. The solutions were stirred and heated to 195–220 °C and held at this temperature for 3–30 hours. The polymerization time correlated with the viscosity of the solution, which was dependent on the solids concentration, polymer molecular weight, and the ratio of the 2,5-py-2COOH monomer to the other diacid monomer. The stir-rate and the temperature were monitored and controlled during the polymerization. Upon reaching an optimal casting viscosity (judged visually), the random copolymer solutions were poured onto a Pyrex or glass plate. Using a doctor's blade, the random copolymer solutions were drawn across the plates to a uniform thickness of 15mil. To drive the formation of gel membranes, the plates and cast films were immediately placed into a humidity controlled chamber at 55% ± 5% relative humidity (RH), 25 ± 2 °C. Due to the hygroscopic nature of the films, complete hydrolysis of the membranes occurred in under 24 hours [7]. The final gel membrane thickness was approximately 300–500 μm.

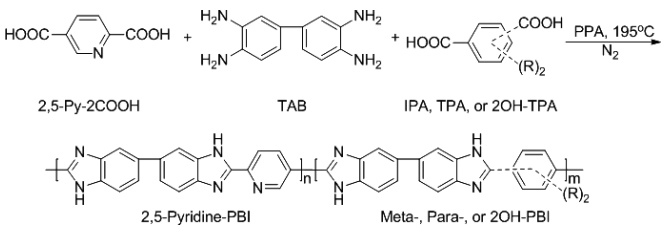

Scheme 1 Synthesis of random copolymers using 2,5-pyridinedicarboxylic acid and 3,3′,4,4′-tetraaminobiphenyl with terephthalic acid (R = H), isophthalic acid (R = H), or 2,5-dihydroxyterephthalic acid (R = –OH).

2.3 Characterization Techniques

Thermogravimetric analysis, differential scanning calorimetry, and inherent viscosity measurements were performed on polymer isolated from the PPA process. Following the polymerization, the polymer/PPA solution that remained in the reaction vessel was hydrolyzed with deionized water. The precipitated polymer was then pulverized in a commercial Waring blender and neutralized with ammonium hydroxide in 500 mL of distilled water. After heating for 1 hour at 100 °C, the polymer was isolated by filtration and washed thoroughly with water to remove any residual ammonium salts. The powder was then dried for 12 hours at 120–130 °C. Thermogravimetric analysis (TGA) was performed with a TA Instruments TGA Q-5000 IR at a constant heating rate of 10 °C min^{-1} under an inert atmosphere. Differential scanning calorimetry (DSC) was performed using a TA Instruments DSC Q-2000 with steady heating and cooling rates of 10 °C min^{-1} and nitrogen flow rate of 20 mL min^{-1}. Following dissolution of the polymer in 96% sulfuric acid at 0.2 g dL^{-1} concentrations, inherent viscosities (IV's) were measured using an Ubbelohde viscometer in a water bath set at 30.0°C. Inherent viscosity was calculated according to Eq. (1).

$$\ln [(t)\,(t_o)^{-1}]\, c^{-1} = \text{Inherent Viscosity (dL g}^{-1}) \quad (1)$$

where t is the solution flow time in seconds, t_o is the solvent (96% sulfuric acid) flow time in seconds, and c is the solution concentration in g dL^{-1}.

The compositions of each film were determined by a multi-step process that was previously described [7, 26]. The phosphoric acid (PA) content within each 2,5-pyridine random copolymer membrane was determined using a Metrohm 716 DMS Titrino autotitrator with a standardized 0.1N sodium hydroxide solution.

Ionic conductivities were measured using four-probe AC impedance spectroscopy. Using an AC Zahner IM6e impedance spectrometer that scanned a frequency range from 1 Hz to 100 kHz, the through-plane bulk measurement of the membrane resistance was recorded. A rectangular sample (3.5 cm × 7.0 cm) was placed in a polysulfone cell with four platinum wire current collectors equally spaced apart. To ensure a through-plane measurement, the two outer electrodes on opposite sides of the membrane set 6.0 cm apart measure the voltage drop across the cell; meanwhile, the two inner electrodes on opposite sides of the membrane set 2.0 cm apart applied current to the cell. Prior to running the ionic conductivity tests, the membranes were preconditioned (dried) in the

polysulfone cell at >100 °C for at least two hours. Eq. (2) was used to calculate proton conductivity:

$$\sigma = (D)\,(L{\cdot}B{\cdot}R)^{-1} \quad (2)$$

where D was the distance between the two inner electrodes, L and B are the membrane thickness and width, respectively, and R was the resistance.

The tensile properties of the membranes were measured using an Instron Tensile Tester (Model 5543A) with a 10 N load cell and crosshead spead of 5 mm/min. Samples were prepared by cutting dog bone specimens (ASTM D683 Type V) from the bulk membrane using a cutting press. All measurements were made at 25 °C ± 3 °C without environmental control on samples preloaded to 0.1N.

The compression creep tests were performed using a TA Instruments RSAIII dynamic mechanical analyzer as described in a previous publication [26]. Membrane samples were prepared by cutting discs with a diameter of 6.3 mm and thickness of approximately 0.9~1.2 mm. Uniform conditioning (drying) was necessary to ensure reproducible results. Prior to the creep compression tests, the sample discs were placed between two parallel smooth Teflon blocks at 180 °C for approximately 24 hours. Conditioning was designed to mirror normal fuel cell operation conditions, during which water evaporated from the membrane samples and an equilibrium composition was reached. During the compression creep tests, a static stress was applied to the sample and held constant for 20 hours and the deformation of the test specimen was recorded as a function of time. All tests were carried out at 180 °C, and the applied stress level was 0.1 MPa. To ensure the compression stress was uniaxial, the compression tool surfaces were coated with PTFE to minimize the friction between the sample and the tool. The strain and stress were recorded as functions of time. The time-dependent strain was divided by the applied stress, and the compliance as a function of time was fitted with the Maxwell model to derive the creep compliance of the film [27]:

$$J(t) = J_s^0 + t \cdot \eta_0^{-1} \quad (3)$$

where J_s^0 represents the steady-state (recoverable) compliance, t is time, and η_0 is the extensional viscosity at zero extension rate.

Membrane electrode assemblies (MEAs) were composed of a random copolymer membrane sandwiched between two electrodes. As described previously, each acid-doped membrane was initially pretreated with concentrated PA to reduce the interfacial resistance of the membrane-catalyst interface [26]. The membrane was then placed between an anode electrode and a cathode electrode and hot-pressed at 150 °C for 90-150 seconds using $2.0{\cdot}10^4$ N (4500 lbs) of force. The target compression for each MEA was 80% of its original thickness. The electrodes contained 1.0 mg/cm^2 platinum (Pt) catalyst loading, had an active area of 45.15 cm^2, and were provided by BASF Fuel Cell, Inc. Anode electrodes contained only Pt as the catalyst, while the cathode electrodes contained a BASF Fuel Cell standard cathode Pt alloy. Fuel cells were assembled in the following order: end plate:PTFE insulator:anode current collector:anode flow field:PTFE gasket:MEA:PTFE gasket:-cathode flow field:cathode current collector:PTFE insulator:-end plate. The fuel cell assembly was clamped, evenly compressed to 5.65 N·m (50 in-lbs) of pressure, and wrapped in an insulating jacket.

Fuel cell performances were measured using 50 cm^2 (active area 45.15 cm^2) single cell stacks from Plug Power or Fuel Cell Technologies. Polarization curves were obtained at atmospheric gas pressures and temperatures ranging from 120–180 °C. Hydrogen was used as a fuel and either air or oxygen gas was used as the oxidant. Prior to the measurement of polarization curves, fuel cells were operated for a break-in period of at least 100 hours at 0.2 A/cm^2 at 180 °C. Long-term steady-state fuel cell tests were performed under constant current (0.2 A/cm^2) and temperature (180 °C) conditions and with a constant flow rate of hydrogen and air. Voltage degradation rates were calculated by a linear fit of cell voltage to time. Product water and PA from the exhaust gases of the anode and cathode were captured by bubbling the gases through distilled water in bottles. The PA loss was determined by analyzing the water in the collection bottles using an ascorbic acid solution and UV-Vis absorbance at 880 nm [28].

3 Results and Discussion

3.1 Synthesis and Characterization of Random Copolymers

Series of 2,5-pyridine-r-meta-PBIs, 2,5-pyridine-r-para-PBIs, and 2,5-pyridine-r-2OH-PBIs were polymerized and cast into gel membranes using the PPA Process. As described in Section 2.2, the polymers were formed via a step-growth polycondensation reaction between aromatic diacids and aromatic tetraamines under acidic conditions. The total amount of diacids was in a 1:1 stoichiometric ratio with the total amount of tetraaminobiphenyl (TAB). The polymerization rate for each copolymer was controlled by adjusting stirring rate and the temperature of the solution. The viscosity of each polymer solution increased as the polymerization proceeded, until an optimal high viscosity for casting was reached. Elemental analysis from a previously reported experiment showed that nitrogen and oxygen content did not deviate over a broad range of monomer conversion, thereby implying that these copolymers are random in composition [26].

Inherent viscosity measurements were performed on the polymer isolated from the PPA Process. More accurate molecular weight characterization techniques were precluded by the insolubility of the polymers in common organic solvents. Inherent viscosities for the random copolymers varied from 0.80 to 2.19 dL g^{-1} for 2,5-pyridine-r-para-PBI, 0.77 to 1.41 dL g^{-1} for 2,5-pyridine-r-meta-PBI, and 0.69 to 1.15 dL g^{-1} for 2,5-pyridine-r-2OH-PBI.This data, along with other polymer and membrane characterization data, can be found in Supplemental Tables S1–S3. Considering the rigid nature of PBI backbones, these polymers range from low-to-moderate molecular weights. The inherent viscosity measurements of these random copolymers were compared with their respective polymerization time. As documented in Supplemental

Tables S1–S3 and as detailed in previous reports [26], shorter polymerization times correlated with lower molecular weights. It is important to note that the solution viscosity determined the polymerization time, and thus, limited the molecular weight of the random copolymers. The relationships between the polymerization solution viscosity with the polymer molecular weight, the chemical composition of the copolymer, and copolymer concentration will be explored in Section 3.2.

Thermal analysis was also performed on the polymer isolated from the PPA Process. Thermogravimetric analysis showed these polymers were stable under an inert atmosphere at temperatures exceeding 450 °C (Supplemental Figure S1). This should not to be confused with membrane gel stability, which will be discussed in Section 3.3. Differential scanning calorimetry of a sample of polymers did not show any transitions below 350 °C (Supplemental Figure S2). The high temperature stability of these polymers is similar to previously synthesized PBIs, and it suggests that these PBIs should also be stable at fuel cell operation temperatures of 180 °C.

3.2 Copolymer Solution Processing into Gel Films

The polymerization solutions were cast directly into membranes by using the PPA Process, as described in the experimental section and in previous publications [7, 26]. Upon reaching an appropriate viscosity suitable for film casting, all of the copolymer solutions were immediately cast onto glass or Pyrex plates using a Gardner blade with a gap space of 15 mil (0.381 mm). These membranes were then placed into a humidity chamber for 12–24 hours to hydrolyze the PPA to PA, which resulted in a membrane that was fully imbibed with PA. All of the chemical compositions of the resulting copolymer membranes are listed in Supplemental Tables S1–S3.

The viscosity of the final polymerization solution plays a critical role in the casting process. If the polymer content or the molecular weight of the polymers were too high, the polymerization solution would be too viscous to flow and could not be cast into thin films. In contrast, a low solution viscosity was an indication of low molecular weight polymers, which if cast into membranes would form mechanically weak films. Identical to the trends observed in a previous paper [26], the viscosities of these copolymer polymerization solutions were directly dependent on the molecular weights of the copolymers, the copolymer ratio, and the concentration of polymer in solution. The relationship between copolymer molecular weight and solution viscosity was visually observed – as the polymerization proceeded, the solution viscosity gradually increased. As the copolymer ratio was changed using monomers with inherently different solubility characteristics, the viscosity increase observed during the polymerization also varied with copolymer ratio. Figure 2 highlights this trend by comparing the para-PBI molar fraction with the polymerization time for an initial monomer charge of 12 wt%. For copolymers with para-PBI molar fractions less than 0.7, polymerizations could be conducted that reached a high solution viscosity suitable for casting. For copolymers with para-PBI molar fractions larger than 0.7, the insolubility of the copolymer did not allow sufficient time for polymerization to high molecular weights and solidification was observed, rendering the polymerization solution unprocessable. Increasing the initial monomer concentration, which thereby increased the polymer concentration in solution, also decreased the amount of time it took to reach an optimal casting viscosity. This was observed through the polymerization of multiple 2,5-pyridine-r-para-PBIs of identical monomer ratios (2,5-py:para = 5:1) but with initial monomer charges ranging from 6-16 wt% – the polymerization times decreasedfrom 16 h to 5.5 h as the monomer charge increased (Supplemental Table S1). These relationships between polymer content or chemical composition with polymerization time were also observed for the 2,5-pyridine-r-meta-PBI and 2,5-pyridine-r-2OH-PBI compositions (Supplemental Tables S2–S3). Generally, 3,5-pyridine random copolymers took longer than their 2,5-pyridine counterparts to reach an optimal casting viscosity [26]. This difference in reaction time is attributed to their relative solubilities in PPA. Thus, the polymerization time required to reach a high viscosity suitable for casting was dependent on the copolymer molecular weight, chemical composition, and overall polymer concentration.

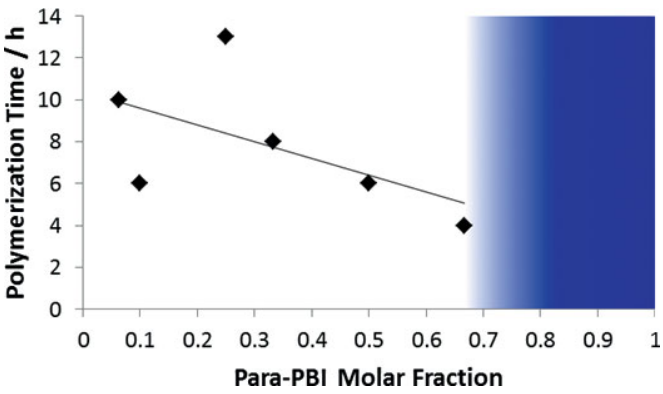

Fig. 2 The polymerization times of a series of 2,5-pyridine-r-para-PBIs with their respective para-PBI molar fraction. All of the polymerizations had an initial monomer charge of 12 wt%. The shaded blue region indicates either a casting process impeded because the solution was too viscous or that the inherent viscosity of the polymer was too low to make a stable membrane.

3.3 Membrane Properties

The structure-property relationships of the membranes from the three copolymer series, 2,5-pyridine-r-2OH-PBI, 2,5-pyridine-r-para-PBI, and 2,5-pyridine-r-meta-PBI, were investigated using a variety of mechanical and electrochemical characterization techniques. The results of these tests were also used to judge the suitability of using these materials as proton exchange membranes in high temperature fuel cells.

Tensile tests were performed on each series of high polymer content membranes at room temperature. The membranes displayed higher Young's moduli than previously reported for low polymer content para-PBI membranes (<1.5 MPa at 25 °C)

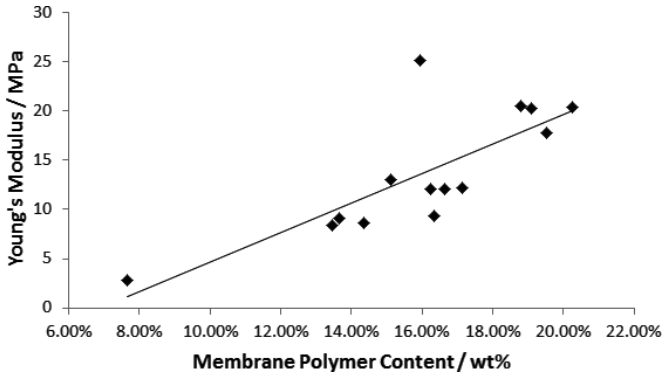

Fig. 3 The Young's moduli of 2,5-pyridine-r-para-PBIs measured in tension at 25 °C ±3 °C on as-cast films. For comparison, low polymer content para-PBI (~5 wt%) has a Young's Modulus less than 1.5MPa under similar testing conditions (data point not shown).

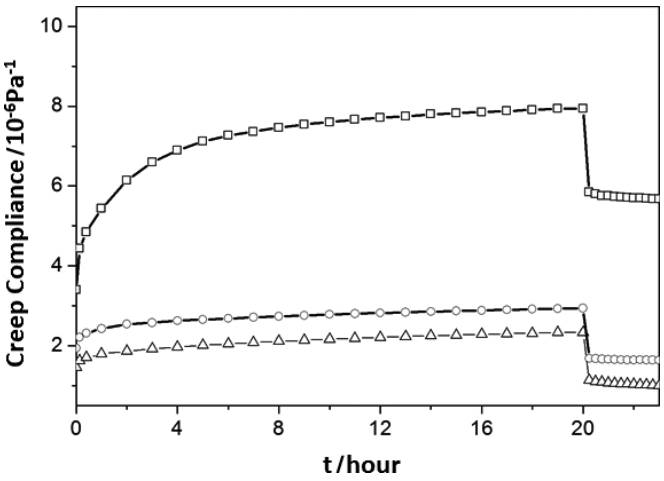

Fig. 4 Creep compliance, J_S^0, curves of a 2,5-pyridine-r-2OH-PBI membrane (MM1-92-3, 13.17 wt% polymer content, triangles), a 2,5-pyridine-r-para-PBI membrane (MM1-40-2, 13.66 wt% polymer content, circles), and a 2,5-pyridine-r-meta-PBI membrane (MM1-72-2, 15.22 wt% polymer content, squares), preconditioned at 180 °C for 24 hours and compressed at 0.1 MPa at 180 °C. Each copolymer is comprised of a 3:1 ratio of 2,5-pyridine-PBI to its counterpart PBI.

[7]. This data is shown in Figure 3 for 2,5-pyridine-r-para-PBI membranes, which shows a linear correlation between polymer content and Young's moduli. This trend is less distinct for the 2,5-pyridine-r-meta-PBI membranes (Supplemental Figure S3), and 2,5-pyridine-r-2OH-PBI membranes (Supplemental Figure S4). The variations in these trends may be due to both the polymer content in the membrane and the limits in molecular weight that can be attained at higher monomer charges. A copolymer ratio higher in 2,5-pyridinedicarboxylic acid improved the solubility of the polymer and thus further assisted in attaining high molecular weights. However, all of the data supports the observation that greater polymer contents in the membranes improves the tensile properties of PBI membranes [26].

Compression creep tests were performed on select high polymer content membranes to investigate the high temperature creep resistance of the gel membranes under static compression. The membranes were preconditioned in an oven at 180 °C for 24 h prior to each test to simulate operational fuel cell conditions and for reproducibility. Figure 4 shows the results of tests for a 2,5-pyridine-r-2OH-PBI membrane, a 2,5-pyridine-r-para-PBI membrane, and a 2,5-pyridine-r-meta-PBI membrane, each composition consisting of a 3:1 ratio of 2,5-pyridine-PBI to its copolymer counterpart. The compliance curves are an average of three experimental data sets under identical preconditioning and testing conditions. As demonstrated in a 20 hour test, the compliance of each membrane increased with time due to material creep under a static compressive force. For each membrane, an initial nonlinear transition period of 1–4 hours was followed by a nearly linear slope compliance period. Upon closer inspection, the compliance slope of the near-linear region gradually decreased over time due to the compression of the gel structure and the resulting composition change. As previously discussed [26], both the creep compliance and creep rate can be used as points of comparison to distinguish a membrane's resistance to creep under static compressive forces. The creep compliance, J_S^0, and the creep rate, dJ/dt, for the high polymer content membranes were much lower than that of para-PBI (~1.0×10^{-5} Pa^{-1} after 20 h and 0.097 MPa^{-1} h^{-1}, respectively).

Table 1 shows the results of the creep tests for the three copolymer membranes. Interestingly, the 2,5-pyridine-r-meta-PBI membrane has the highest creep compliance and creep rate, even though it had the highest polymer content. This indicates that the creep compliances and rates are not solely based on polymer content, but are also influenced by chemical composition. Based on the results of J_S^0, η_0, and dJ/dt, 2,5-pyridine-r-meta-PBI membranes displayed the lowest creep resistance, while 2,5-pyridine-r-para-PBI membranes and 2,5-pyri-

Table 1 Creep compliance test results for three different copolymer systems with a 3:1 ratio of 2,5-pyridine-PBI to its counterpart PBI.

Membrane Type	Polymer Content (wt%)	J_S^0 (10^{-6} Pa^{-1})	η_0 (10^{12} Pa s)	J at 20h (10^{-6} Pa^{-1})	dJ/dt_{8-20h} 10^{-6} Pa^{-1} hr^{-1})
2,5-pyridine-r-2OH-PBI	13.17	1.35±0.20	0.15±0.04	2.33±0.32	0.0180±0.0005
2,5-pyridine-r-para-PBI	13.66	1.34±0.34	0.18±0.06	2.94±0.77	0.0167±0.0002
2,5-pyridine-r-meta-PBI	15.22	2.26±0.63	0.08±0.06	7.94±2.60	0.0384±0.0004

J_S^0 = Steady-state recoverable compliance
η_0 = Extensional viscosity at zero extension rate
J = Compliance
dJ/dt_{8-20h}= Creep rate (change in compliance over the last 12 hours of the test)

dine-r-2OH-PBI membranes showed significantly improved resistance. Based on the results of creep compliance at 20 h, 2,5-pyridine-r-2OH-PBI membranes showed slightly better creep resistance than 2,5-pyridine-r-para-PBI membranes. At the end of the compression creep test, the J_S^0 and η_0 values of 2,5-pyridine-r-2OH-PBI and 2,5-pyridine-r-para-PBI membranes were comparable within the range of experimental error, suggesting that adding the 2OH- and para- comonomers have a similar reinforcing effect. The results of these tests correlate with the relative solubility of these membranes in PA (see Figure 1) and suggest a correlation with polymers possessing a more extended chain conformation. Thus, the less-soluble PBI components (e.g. 2OH- or para-PBI) impart higher gel thermal stabilities on membranes than more-soluble PBI components (e.g. meta-PBI).

Due to its accuracy and ease of measurement, proton conductivity is a common metric used to compare the relative merits of proton exchange membranes. Perfluorosulfonic acid-based PEMs, such as DuPont's Nafion, depend on water as a dopant to facilitate proton conduction. Due to hydration issues with the membrane, proton conductivities are generally very low at temperatures exceeding 100 °C. In contrast, PA-doped PBI membranes display much higher proton conductivities at elevated temperatures due to the low vapor pressure of PA and the faster proton-transport kinetics of phosphoric acid [29–31]. Prior investigations of high temperature fuel cell membranes have shown that water content, phosphoric acid content, membrane morphology, and membrane chemistry all significantly affect the proton conductivity measurements [9, 16, 17].

Proton conductivity was measured using four-probe, through-plane a.c. impedance spectrometry. To simulate anhydrous fuel cell operating conditions, as-cast copolymer membranes were dehydrated by preconditioning the membranes at 180 °C for approximately two hours. Figure 5 shows proton conductivity and PA content of 2,5-pyridine-r-para-PBI membranes as functions of polymer content (wt%). The correlation of the data sets indicates that proton conductivities generally increase with higher PA content for these copolymer membranes (see also Supplemental Figure S5). This agrees with the general trends reported in literature, e.g., that PBI membranes with greater concentrations of phosphoric acid display greater proton conductivities.[14, 26] Similar trends were found for both 2,5-pyridine-r-meta-PBIs and 2,5-pyridine-r-2OH-PBIs (Supplemental Tables S2 and S3). By changing the initial monomer concentration of the polymerization solution, the PA content (and thus the proton conductivity) of these membranes could be moderately controlled.

A series of non-optimized fuel cell tests were performed to further investigate the electrochemical properties of the 2,5-pyridine high solids MEAs (Figure 6). Visual inspection of the

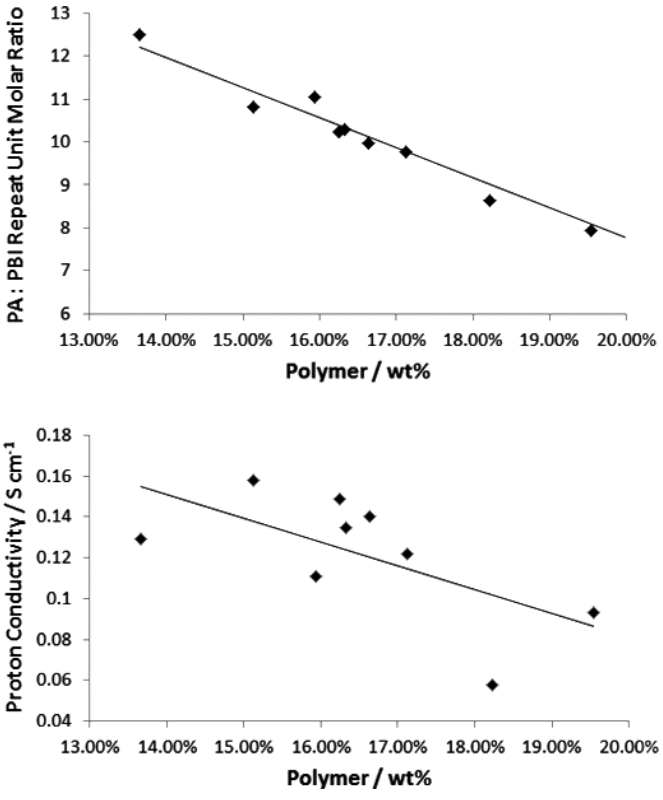

Fig. 5 The PA content of as-cast 2,5-pyridine-r-para-PBI membranes (top). Following preconditioning for 2h at 180 °C, the membrane's anhydrous proton conductivities were measured at 180 °C (bottom).

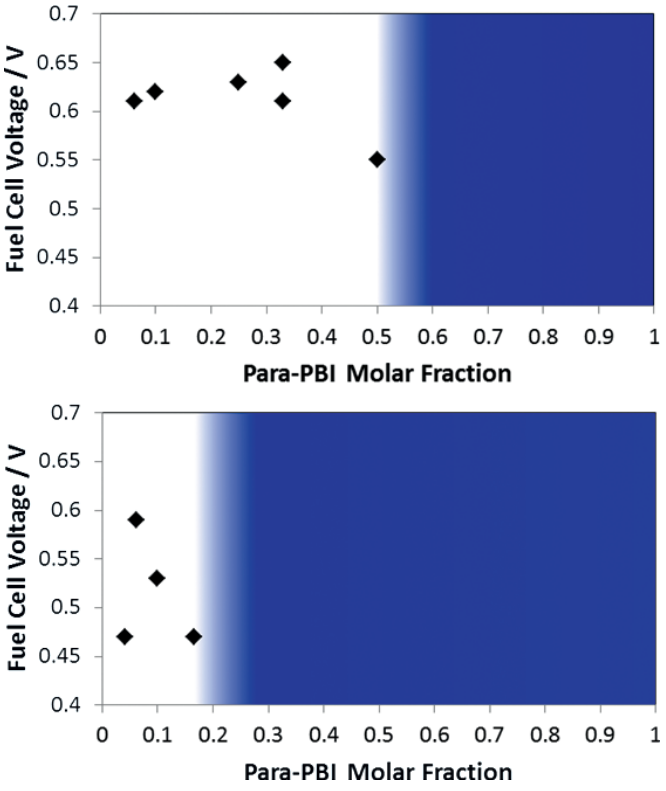

Fig. 6 Processing map and non-optimized fuel cell performances at 0.2 A cm^{-2} using H_2:Air at a 1.2:2.0 stoichiometric ratio (following break-in) at 180 °C of 2,5-pyridine-r-para-PBI gel films. Membranes were cast from 12 wt% monomer charge (top) and 16 wt% monomer charge (bottom) solutions. The shaded blue regions represent copolymers which were too viscous to cast or too low in molecular weight to form mechanically stable membranes.

hot-pressed MEAs and fuel cell performance indicated that all of the high polymer content 2,5-pyridine membranes were thermally stable at least up to 150 °C. These dramatically contrast with 3,5-pyridine copolymer membranes, which showed thermal instability at 150 °C with high 3,5-pyridine-PBI proportions [26]. However, it was determined that only specific ratios of 2,5-py-2COOH to IPA, TPA, or 2OH-TPA were feasible to polymerize and cast into membranes. High copolymer ratios of the meta-, para-, or 2OH- functionalized PBIs correlated with decreased polymerization times and reduced solubility in PPA (Figure 2). Copolymers with poor solubility resulted in either highly viscous solutions that could not be easily cast into membranes or low molecular weight polymers that formed mechanically unstable films. Figure 6 shows the effects of monomer ratios and polymer solution concentrations with solution processability and fuel cell performance for a series of 2,5-pyridine-r-para-PBI membranes. These performance-processing maps indicate processing windows where mechanically-stable membranes could be cast. The shaded blue regions of the figure represent compositions yielding polymerization solutions that did not lead to usable cast films. Polymerization solutions with a 12 wt% monomer charge required a 50% 2,5-pyridine-PBI composition, meanwhile those with a 16 wt% monomer charge needed at least 80% 2,5-pyridine-PBI. This data supports our claim that higher polymer content membranes can be cast using more soluble PBIs.

Long-term steady-state fuel cell tests were performed on a membrane of each series of high solids content 2,5-pyridine copolymer membranes. These tests were performed at 180 °C, 0.2 A cm^{-2}, and using H_2:Air at a 1.2:2.0 stoichiometric ratio. Figure 7 shows the voltage response at constant current density and acid loss data for a 2,5-pyridine-r-meta-PBI membrane (MM1-72-4 in Supplemental Table S2). Following an initial break-in period of 150 h, the fuel cell recorded a voltage degradation rate of 9.45 μV h^{-2} that was much lower than a low-solids para-PBI membrane (60 μV h^{-1}) at 190 °C [11]. The lower voltage degradation rate could partially be due to operation at a lower temperature. Additionally, the total PA loss rate for this cell (5.55 ng cm^{-2} h^{-1}) is the lowest for any PBI fuel cell recorded to date, and is over an order of magnitude lower than the PA loss rate of para-PBI (110.4 ng cm^{-2} h^{-1} at 190 °C). The amount of PA lost from the cathode was higher than that lost from the anode, which is likely an effect of the water generation process at the cathode. Similarly, Figure 8 shows the performance and acid loss of a 2,5-pyridine-r-para-PBI membrane (MM1-46-4). The voltage degradation rate of this MEA was 6.75 μV h^{-1}, which is again much lower than para-PBI at 190 °C. However, the total PA loss rate of this membrane (94.73 ng cm^{-2} h^{-1}) was much closer to that of para-PBI. This high PA loss rate was partially attributed to the poor mechanical properties observed in the room temperature tensile tests (the strain-at-break for this membrane occurred at 16% elongation). For both of these fuel cells, the PA loss rate from the high solids content MEA's suggests that PA loss will not be a major factor of fuel cell failure.

Similar testing was conducted on 2,5-pyridine-r-2OH-PBI (MM1-92-2, 14.99% polymer content in as-cast membrane) membrane subjected to a long-term steady-state fuel cell test at 180 °C, 0.2 A cm^{-2}, and using H_2:Air at a 1.2:2.0 stoichiometric ratio (Supplemental Figure S6). This MEA was operated for more than 8600 h and exhibited a voltage degradation rate of 6.15 μV h^{-1}, also supporting the claim that high solids membranes are suited for extended lifetime electrochemical applications. As previously described, polymer electrolyte membranes consisting of polymers with low solubilities in PPA (e.g. 2OH-PBI) and high polymer content often result in membranes with enhanced creep resistance. The enhanced stability of the membrane could contribute to the low voltage degradation rate of the MEA; however, additional tests are necessary

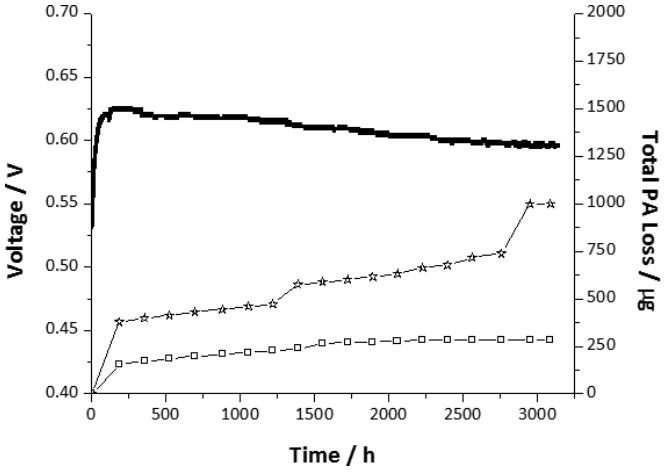

Fig. 7 Long-term steady-state performance (upper line) of a 2,5-pyridine-r-meta-PBI (MM1-72-4) copolymer membrane at 0.2 A cm^{-2}, 180 °C, and using H_2:Air at a 1.2:2.0 stoichiometric ratio. Solids Content = 19.09 wt%. Anode PA loss (squares) = 0.93 ng cm^{-2} h^{-1}, Cathode PA loss (stars) = 4.62 ng cm^{-2} h^{-1}, voltage degradation rate = 9.45 μV h^{-1}.

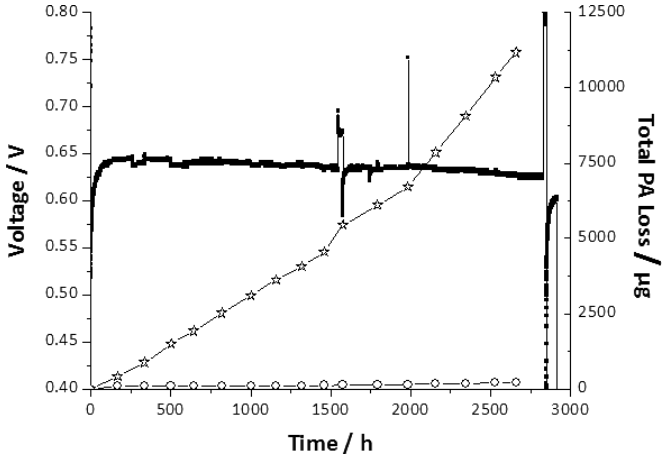

Fig. 8 Long-term steady-state performance of a 2,5-pyridine-r-para-PBI (MM1-46-4) copolymer membrane at 180 °C, 0.2 A cm^{-2}, and using H_2:Air at a 1.2:2.0 stoichiometric ratio. Anode PA Loss (circles) = 1.69 ng cm^{-2} h^{-1}, Cathode PA Loss (stars)= 93.04 ng cm^{-2} h^{-1}, voltage degradation rate = 6.75 μV h^{-1} following 150h break-in. Polarization curve was taken at 1500 h, as shown by the peak in the graph. Significant fuel cell voltage loss (~0.03V) was observed after 2750 h due to an unplanned station event.

to verify the relationship between membrane creep resistance and long-term fuel cell performance.

4 Conclusions

Three series of high polymer content membranes – 2,5-pyridine-r-meta-PBI, 2,5-pyridine-r-para-PBI, and 2,5-pyridine-r-2OH-PBI – were polymerized and cast into membranes using the PPA process. By adjusting the ratio of the more-soluble pyridine monomer to the less-soluble IPA, TPA, or 2OH-TPA counterpart, the solubility of the resulting copolymer, and thus, its processability into a PA-doped membrane could be controlled. Both the monomer concentration and ratio of monomers were used to construct processing maps to describe copolymer compositions that could form stable membranes for electrochemical applications.

All membranes produced within the defined processing windows were thermally stable at 180 °C. Measurement of the compressive creep properties of the membranes at 180 °C showed that membranes consisting of lower solubility copolymers and high solids membrane contents had reduced creep compliances at high temperatures under static loads. Thus, copolymer compositions were identified with sufficient processing capabilities and high temperature gel stability for further investigation. Many high solids compositions were identified that exhibited proton conductivities greater than 0.1 S cm^{-1}, even with reduced PA content.

Long-term steady-state fuel cell tests performed on the high polymer content membranes were compared to previous results for low polymer content para-PBI membranes. Much lower voltage degradation rates ranging from 6.15–9.45 μV h^{-1} were observed for the 2,5-pyridine copolymer membranes at 180 °C, as compared with 60 μV h^{-1} for para-PBI reported at 190 °C. PA loss rates were found to be quite low and suggested that PA loss is not likely to act as a primary failure mode during steady-state operation.

Acknowledgements

The authors would like to gratefully acknowledge BASF Fuel Cell, Inc., Dr. Gordon Calundann, and Dr. Joerg Belack for technical and financial support of the work. The authors also acknowledge DARPA for partial support of this research.

References

[1] A. Chandan, M. Hattenberger, A. El-Kharouf, S. Du, A. Dhir, V. Self, B. G. Pollet, A. Ingram, W. Bujalski, *J. Power Sources* **0000**, *231*, 264–278.

[2] D. Dunwoody, J. Leddy, *The Electrochemical Society Interface* **2005**, *3*, 37–39.

[3] H. A. Vogel, C. S. Marvel, *J. Polym. Sci.* **1961**, *50*, 511–539.

[4] H. A. Vogel, C. S. Marvel, *J. Polym. Sci., Part A1* **1963**, *1*, 1531–1541.

[5] J. S. Wainright, J. T. Wang, D. Weng, R. F. Savinell, M. Litt, *J. Electrochem. Soc.* **1995**, *142 (7)*, L121–L123.

[6] M. Litt, R. Ameri, Y. Wang, R. F. Savinell, J. S. Wainright, *Mater. Res. Soc. Symp. Proc.* **1999**, 313–323.

[7] L. Xiao, H. Zhang, E. Scanlon, L. S. Ramanthan, E. W. Choe, D. Rogers, T. Apple, B. C. Benicewicz, *Chem. Mater.* **2005**, *17 (21)*, 5328–5333.

[8] S. Yu, B. C. Benicewicz, *Macromolecules* **2009**, *42 (22)*, 8640–8648.

[9] M. Molleo, T. J. Schmidt, B. C. Benicewicz, *Polybenzimidazole-Phosphoric Acid (PBI-PA)-Based Fuel Cells, Encyclopedia of Sustainability, Science and Technology*, Springer Science + Business Media LLC, New York, **2012**, pp. 391–431.

[10] L. Xiao, H. Zhang, T. Jana, E. Scanlon, R. Chen, E. W. Choe, L. S. Ramanthan, S. Yu, B. C. Benicewicz, *Fuel Cells* **2005**, *5 (2)*, 287–295.

[11] S. Yu, L. Xiao, B. C. Benicewicz, *Fuel Cells* **2008**, *8 (3–4)*, 165–174.

[12] G. Qian, B. C. Benicewicz, *J. Polym. Sci., Part A* **2009**, *47 (16)*, 4064–4073.

[13] J. Mader, B. C. Benicewicz, *Macromolecules* **2010**, *43*, 6706–6715.

[14] D. C. Seel, B. C. Benicewicz, L. Xiao, T. J. Schmidt, High-temperature Polybenzimidazole-based Membranes, in *Handbook of Fuel Cells*, **2009**, *5*, pp. 300–312.

[15] Q. Li, R. He, J. Gao, O. J. Jensen, N. J. Bjerrum, *J. Electrochem. Soc.* **2003**, *150 (12)*, A1599–A1605.

[16] R. He, Q. Li, G. Y. Xiao, N. J. Bjerrum, *J. Membr. Sci.* **2003**, *226 (1–2)*, 169–184.

[17] Q. Li, H. A. Hjuler, N. J. Bjerrum, *J. Appl. Electrochem.* **2001**, *31 (7)*, 773–779.

[18] J. Mader, X. Lixiang, T. Schmidt, B. C. Benicewicz, *Adv. Polym. Sci.* **2008**, *216*, 63–124.

[19] T. J. Schmidt, J. Baurmeister, *ECS Transactions* **2006**, *3 (1)*, 861–869.

[20] Y. Garsany, B. D. Gould, O. A. Baturina, K. E. Swider-Lyons, *Electrochemical and Solid-State Letters* **2009**, *12 (9)*, B138–B140.

[21] U.S. Dept. Energy, An Integrated Strategic Plan for the Research, Development, and Demonstration of Hydrogen and Fuel Cell Technologies, 2011. Available at http://www1.eere.energy.gov/hydrogenandfuelcells/pdfs/program_plan2011.pdf

[22] A. Suvorov, J. Elter, R. Staudt, R. Hamm, G. Tudryn, L. Schadler, G. Eisman, *International Journal of Solids and Structures* **2008**, *45 (24)*, 5987–6000.

[23] K. A. Patankar, D. A. Dillard, S. W. Case, M. W. Ellis, Y.-H. Lai, C. S. Gittleman, *Fuel Cells* **2012**, *12 (5)*, 787–799.

[24] Y.-H. Lai, C. K. Mittelsteadt, C. S. Gittleman, D. A. Dillard, *J. Fuel Cell Sci. Technol.* **2009**, *6 (2)*, 021002–021013.

[25] Y. Li, D. A. Dillard, S. W. Case, M. W. Ellis, Y.-H. Lai, C. S. Gittleman, D. P. Miller, *J. Power Sources* **2009**, *194 (2)*, 873–879.

[26] M. A. Molleo, X. Chen, H. J. Ploehn, K. J. Fishel, B. C. Benicewicz, *Fuel Cells* **2014**, *14 (1)*, 16–25.

[27] J. D. Ferry, *Viscoelastic Properties of Polymers*, 3rd Ed., John Wiley & Sons, New York **1980**.
[28] Standard methods for the examination of water and wastewater **1999**, Available at http://www.scribd.com/doc/44520215/Standard-Methods-for-the-Examination-of-Water-and-Waste-Water-20th-1999.
[29] L. Vilciauskas, S. J. Paddison, K.-D. Kreuer, *J. Phys. Chem. A* **2009**, *113*, 9193–9201.
[30] T. Dippel, K. D. Kreuer, J. C. Lassegues, D. Rodriguez, *Solid State Ionics* **1993**, *61*, 41–46.
[31] A. Bozkurt, M. Ise, K. D. Kreuer, W. H. Meyer, G. Wegner, *Solid State Ionics* **1999**, *125*, 225–233.

